TORSION STRAIN EFFECTS ON CRITICAL CURRENTS OF HTS SUPERCONDUCTING TAPES

Makoto Takayasu, Joseph V. Minervini, and Leslie Bromberg

Massachusetts Institute of Technology
Plasma Science and Fusion Center
Cambridge MA, 02139, USA

ABSTRACT

A torsional twist strain effect on the critical current of a thin HTS tape has been found to be well described by a longitudinal strain model taking into account the internal shortening compressive strains accompanied with the tensile longitudinal strains due to a torsional twist. The critical current of a twisted tape is given by the integration of the critical current densities corresponding to the strain distribution over the tape cross-section using axial strain data of the tape. The model is supported with experimental results of YBCO and BSCCO-2223 tapes. It has been also found that torsional twisting effects on the critical currents of a tape composing of the conventional lapped-tape cable and the twisted stacked-tape cable are described by the same equation as that of a twisted single tape.

KEYWORDS: Torsion, twist, cabling, tape cable, critical current, high temperature superconductor, HTS cable.

INTODUCTION

Conventional transmission cables have been made of multiple HTS tapes lapped concentrically on a central former and enclosed in a tube cryostat [1, 2]. Most HTS tape devices have been composed of a single tape or only a few tapes in parallel. Very few cabling methods of HTS tapes have been developed. One of those is Roebl cabling which has been demonstrated for a 2 kA conductor [3]. It is a good method to reduce AC losses, however it will not be easy to scale up.

YBCO tapes (second generation HTS tapes) have excellent high current capabilities at high magnetic fields [4]. At present no comparable superconducting material has been found. Recently the field-orientation degradation (critical current anisotropy) of YBCO tapes has been substantially improved by SuperPower, Inc using a REBCO HTS film technique substituted with Gd and Zr [5]. The reduced field-orientation sensitivity increases design flexibilities of HTS tape applications.

We have developed a new cabling method of HTS tapes. Stacked flat tapes are twisted along the axis of the stack. This cabling method is conceptually different from the existing lapped type cabling. The method allows developments of high current, compact conductors for various applications such as power transmission cables and high field magnets.

In order to determine fabrication degradations for HTS flat tape cablings and also to develop better cable processing methods, it is desired to understand the mechanical properties of HTS tapes, especially torsion strain phenomena. Torsion studies of HTS tapes are very limited [6-8]. In this paper, analytical models of the torsion twist strains for an HTS tape are presented including those for tapes in both lapped-tape and stacked-tape cables. The calculated torsional strains are correlated to the corresponding axial strains of the tapes. The model results are compared with critical current measurement of twisted BSCCO and YBCO HTS tapes. Characterizations of the critical currents under a wide range of torsional strains were carried out at 77 K to determine the critical current degradation due to these mechanical strains. Irreversible degradation of the critical current due to applied torsion was also evaluated, as well as the effect of torsion cycling.

LONGITUDINAL STRAIN IN TWISTED TAPE

FIGURE 1 shows schematic illustrations of a twisted single flat tape, a conventional lapped-tape cable and a twisted stacked-tape cable.

When a torsional twist of the angle ϕ is applied to a thin rectangular tape (width w and thickness t) of the length L as shown in FIGURE 1a, the longitudinal chord $\overline{AB_1}$ parallel to the z-axis at the distance x (y=0) from the z-axis elongates to $\overline{AB_2}$, and the length is given by

$$\overline{AB_2} = \sqrt{L^2 + (x\phi)^2} = L\sqrt{1 + \left(\frac{x\phi}{L}\right)^2} \approx L\left\{1 + \frac{1}{2}\left(\frac{x\phi}{L}\right)^2\right\} \tag{1}$$

Therefore the tensile axial longitudinal strain ε_t of the chord $\overline{AB_2}$ due to the torsional twist is obtained as [1]

$$\varepsilon_t = \frac{\overline{AB_2} - \overline{AB_1}}{\overline{AB_1}} = \frac{L\left\{1 + \frac{1}{2}\left(\frac{x\phi}{L}\right)^2\right\} - L}{L} = \frac{1}{2}\left(\frac{x\phi}{L}\right)^2 = \frac{x^2\theta^2}{2} \tag{2}$$

where θ is the twist angle per unit length ($\theta = \phi/L$).

In the application of a torsional twist to a tape it is assumed that the tape does not have net force in the longitudinal direction. That is, the longitudinal tensile force due to the torsional strain results in the shortening of the tape and zero net internal longitudinal force in the tape [9, 10]. The compressive strain ε_0 is established in the tape. It is determined from the condition that the integrated longitudinal force (and thus strains) over the tape cross-section is to be zero [9]. The integrated force of the total stress $\sigma_x = E\,\varepsilon_t + E\,\varepsilon_o$ (E is Young's modulus.) due to the tensile longitudinal strain ε_t of equation (2) and the shortening contraction ε_o is given as follows, and should be zero.

$$\int_{-\frac{w}{2}}^{\frac{w}{2}} t\sigma_x dr = t\int_{-\frac{w}{2}}^{\frac{w}{2}} E\left\{\frac{\theta^2 x^2}{2} + \varepsilon_o\right\}\cdot dx = 0 \tag{3}$$

From this equation, the compressive strain ε_o is obtained as

$$\varepsilon_o = -\frac{\theta^2 w^2}{24} \tag{4}$$

(a)   (b)   (c)
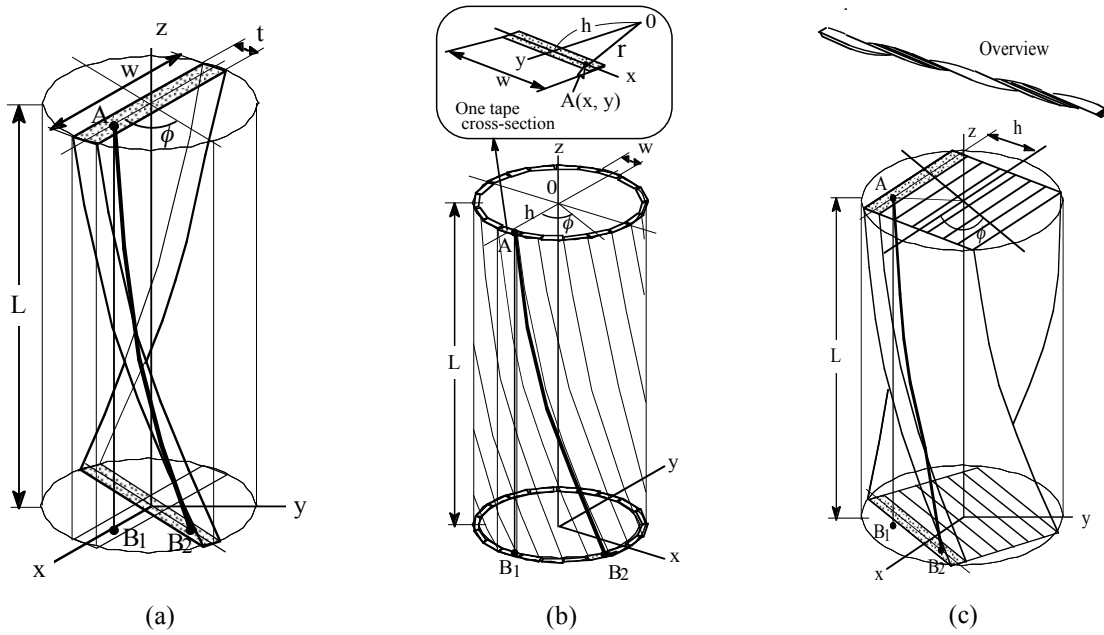
FIGURE 1. Schematic illustrations of (a) a single twisted thin rectangular tape, and two types of HTS tape cables: (b) Conventional lapped-tape cable, and (c) Twisted stacked-tape cable.

Now the actual longitudinal strain ε_x of the summation of the tensile strain ε_t and the shortening compressive strain ε_0 is given as a function of the distance x,

$$\varepsilon_x = \varepsilon_t + \varepsilon_o = \frac{\theta^2}{2}\left(x^2 - \frac{w^2}{12}\right) \tag{5}$$

Equation (5) shows the actual longitudinal strains in the tape, which are compressive in the region of $-w/(2\sqrt{3}) < x < w/(2\sqrt{3})$ and tensional in $w/(2\sqrt{3}) < |x| < w/2$.

Commonly the shear strain and stress are used for torsional twisting mechanics [6-8, 11]. The shear strain γ_{xz} in the twisted narrow rectangular cross-section tape is given $\gamma_{xz} = 2\theta y$ for the tape shown in FIGURE 1a. The maximum shear strain γ_{max} in the tape is written as $\gamma_{max} = \theta t$ which occurs in the middle portion of the long surface of the rectangular tape surface [11]. Using the maximum shear strain $\gamma_{max} = \theta t$, the longitudinal strain ε_x of equation (5) and its maximum and minimum values are written as;

$$\varepsilon_x = \frac{1}{2}\left(\frac{\gamma_{max}}{t}\right)^2\left(x^2 - \frac{w^2}{12}\right) \tag{6}$$

$$\varepsilon_{max} = \frac{w^2\theta^2}{12} = \frac{w^2}{12}\left(\frac{\gamma_{max}}{t}\right)^2 \quad \text{at the far ends } (x=\pm w/2) \tag{7}$$

$$\varepsilon_{min} = -\frac{w^2\theta^2}{24} = -\frac{w^2}{24}\left(\frac{\gamma_{max}}{t}\right)^2 \quad \text{at the tape center } (x=0) \tag{8}$$

Since superconducting area in an HTS tape is engaged with large amount of various material of substrate or reinforcement clad, it is difficult to define the thickness for obtaining the maximum shearing strain γ_{max}. The longitudinal strain equation (5) is independent upon the thickness of the tape; therefore equation (5) is better for the analysis of a thin rectangular HTS tape than equation (6).

FIGURE 1b shows a schematic illustration of a conventional HTS cable composed of

multiple tapes lapped circumferentially on a cylindrical surface. A novel conductor concept that is assembled with a stack of HTS tapes illustrated in FIGURE 1c. The stacked conductor is twisted about a longitudinal axis of the stack. During the cabling processes of the conventional lapped-tape and stacked-tape cables, the HTS tapes experience torsional twisting strains. The axial longitudinal strains in both cases shown in FIGURES 1b and 1c are mathematically treated in the same way. Therefore the following analyses are applied to both cases.

For a torsional twist of the twist angle θ ($\theta = \phi/L$), the tensile longitudinal strain ε_{txh} of the chord $\overline{AB_1}$ in a tape located at the distance y=h from the cable center (the z-axis) shown in FIGURES 1b and 1c is given from the analogy of equation (2) in the single tape analysis:

$$\varepsilon_{txh}(y = h) = \frac{1}{2}\theta^2 \left(x^2 + h^2\right) \tag{9}$$

where h is the distance of the tape location from the z-axis.

Since longitudinal forces are not applied to any tapes during lapping or twisting during cabling, the net longitudinal force of each tape must be zero at equilibrium as in the case of a single twisted tape. From the force balance accompanying the shortening compressive strain ε_{oh} for each tape,

$$\int_{-\frac{w}{2}}^{\frac{w}{2}} t\left(\varepsilon_{txh} + \varepsilon_{oh}\right) dr = t \int_{-\frac{w}{2}}^{\frac{w}{2}} E\left\{\frac{1}{2}\theta^2\left(x^2 + h^2\right) + \varepsilon_{oh}\right\} dr = 0 \tag{10}$$

From this equation the shortening compressive internal strain ε_{oh} in a tape is given by

$$\varepsilon_{oh} = -\frac{\theta^2}{2}\left(\frac{w^2}{12} + h^2\right) \tag{11}$$

The longitudinal strain ε_{xh} of a tape in both lapped-tape and stacked-tape cables is thus given by

$$\varepsilon_{xh} = \varepsilon_{txh} + \varepsilon_{oh} = \frac{1}{2}\theta^2\left(x^2 + h^2\right) - \frac{\theta^2}{2}\left(\frac{w^2}{12} + h^2\right) = \frac{\theta^2}{2}\left(x^2 - \frac{w^2}{12}\right) = \varepsilon_x \tag{12}$$

Equation (12) shows that the actual longitudinal strain ε_{xh} is equal to that of a twisted single-tape and it does not depend on the tape location h in the y-direction. Therefore any tapes in both lapped-tape and stacked-tape cables experiences the exactly same longitudinal strain distribution as that of the single twisted tape given by equation (5).

CRITICAL CURRENT ANALYSIS OF TWISTED TAPE

The critical current is a function of the axial longitudinal strain. Since the longitudinal strains are not constant, but distribute in a twisted tape, the critical current I_c of a twisted tape is written by a summation of critical current densities $j_c(\varepsilon_x)$ over the tape cross-section of the width w and the thickness t_s, corresponding to the strain distribution given by equation (5);

$$I_c = t_s \int_{-\frac{w}{2}}^{\frac{w}{2}} j_c(\varepsilon_x) dx \tag{13}$$

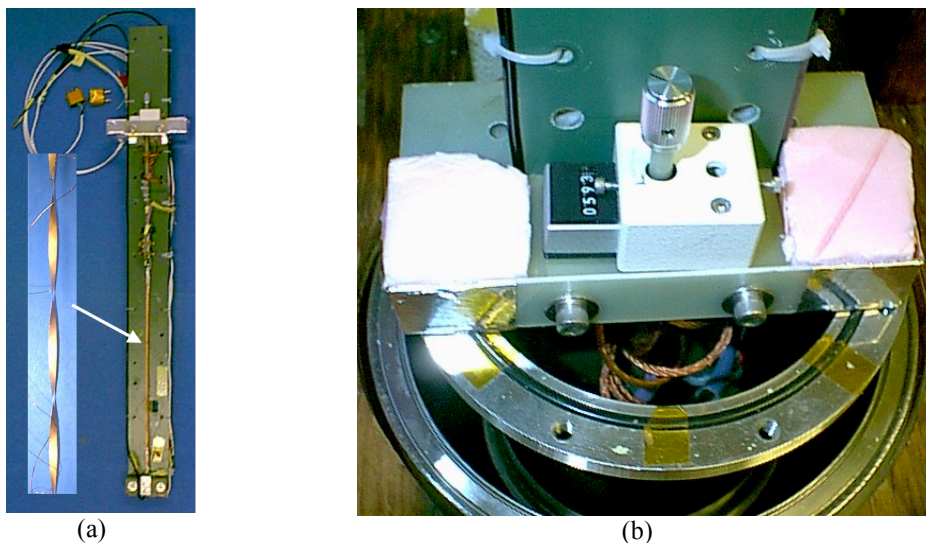(a)   (b)

FIGURE 2. (a) Overview of a torsion test probe on a G10 plate of 915 mm height, 76 mm width and 6 mm thick. Test tape of a 300 mm section is twisted by rotating the upper current lead. The insert shows an enlarged twisted tape. (b) The probe is in a Dewar. A counter on a top flange measures the twisting angle.

The critical current density $j_c(\varepsilon)$ for an axial strain ε is obtained from critical current data $I_c(\varepsilon)$ of axial strain tests; $j_c(\varepsilon) = I_c(\varepsilon)/(t_s w)$.

TORSIONAL TWIST TEST METHOD

FIGURE 2a shows a torsion device to test a 380 mm long HTS tape that includes 40 mm terminations at both ends to a copper lead. The 300 mm test-section had two sets of voltage taps. The voltage tap separations were 100 mm and 200 mm. The lower termination of the sample is fixed, while the upper termination was mounted on a rotatable rod which was connected to a counter to measure the rotation with a resolution of 1 degree. The insert in FIGURE 2a shows a twisted sample with voltage tap wires. Torsion experiments were performed with YBCO and BSCCO-2223 tapes under varying torsion; tests were performed in liquid nitrogen (77 K) in the absence of externally applied magnetic field. The YBCO tape was a 2G Type SCS 4050 on 50 μm nickel alloy (Hastelloy®) substrate with a surrounding copper stabilizer (made by SuperPower, Inc.). The tape width and thickness were 4.05 mm and 0.128 mm, respectively. The BSCCO tape was a PIT-processed Bi-2223 in a silver alloy matrix with a clad of 35 μm stainless steel reinforcement on both sides (made by American Superconducting Co., AMSC). The tape width and thickness were 3.05 mm and 0.249 mm, respectively. The BSCCO samples were the same used for the levitating coil of the Levitated Dipole Experiment (LDX) [12].

CRITICAL CURRENT TEST RESULTS

Critical current test results of the YBCO sample for various torsions are shown in FIGURE 3. The critical current normalized to the critical current of the undisturbed tape (86.5 A) is plotted as a function of the twist pitch in FIGURE 3a. The criterion of the critical current was 100 μV/m. During application of the torsion (Torsion Up 1st cycle), the twist pitches was decreased to 100 mm, and then the twist pitches were increased to 1000 mm (Torsion Down 1st cycle). The normalized critical currents in the 1st cycle are plotted with solid and open circles in the figure. It is noted that the critical currents slightly

increased with increasing torsion and then sharply decreased for twist pitches below 130 mm. The triangles in the figure shows the test results of 2nd cycle, where the twist pitches were decreased to 89 mm (Torsion UP 2nd cycle) and then the torsions were decreased to a twist pitch of 1000 mm (Torsion Down 2nd cycle). No permanent degradation of the current density was observed after the two-cycle processes. The n-values of the critical current ($V \propto I^{n}$), obtained at the criteria of 100 µV/m and 1000 µV/m, are shown in FIGURE 3b. The n-values showed a tendency of decreasing very slightly during the two-cycle torsion process, but the n-values were ~32 consistently without significant torsion effects.

In FIGURE 3a, the bold line shows an analytical behavior obtained with equations (5) and (13) by using the published axial longitudinal strain data of SuperPower YBCO [13]. The data of the critical current vs. axial strain were approximated by the following polynomial equation to perform the integration in equation (13);

$$I_c/I_o = 0.057713 \times 10^{12}\, \varepsilon_x^{6} - 0.03979215 \times 10^{10}\, \varepsilon_x^{5} - 0.2090279 \times 10^{8}\, \varepsilon_x^{4}$$
$$+ 0.02385557 \times 10^{6}\, \varepsilon_x^{3} - 0.1668065 \times 10^{4}\, \varepsilon_x^{2} - 0.003662115 \times 10^{2}\, \varepsilon_x + 1 \qquad (14)$$

The integration in equation (13) was carried out by the Gaussian integration method of order 40 using Microsoft Excel®. The calculated curve, as seen in FIGURE 3a, agreed very well with the experimental results. The critical currents increased by torsion above the twist pitch of about 150 mm may be due to the residual strain release with the torsional twist. The residual strain releasing effect was not included in the present analysis.

Test results of BSCOO tapes are shown in FIGURE 4. The critical currents normalized to the initial critical current of the undisturbed tape (69.4 A for the 1st sample and 67.4 A for the 2nd sample) are plotted as a function of the twist pitch in FIGURE 4a. Two samples obtained from the same spool were tested. During the application of the torsion, the torsion of one sample (open circles) was released once at a twist pitch of 103 mm, while for the other sample (crosses) it was released 9 times as shown in the figure. The data clearly showed that the degradations due to the twisting did not recover after the torsion strains were released. The torsion or strain seems to create permanent damage. As seen in FIGURE 4, the degradation of the critical current sharply increased for twist pitches shorter than 200 mm. A bold line in FIGURE 4 shows an analytical result obtained from equations (5) and (13). In the analysis the critical currents of the BSCCO as a function of the axial strain were approximated by the following empirical equations [14] for the integration of equation (13);

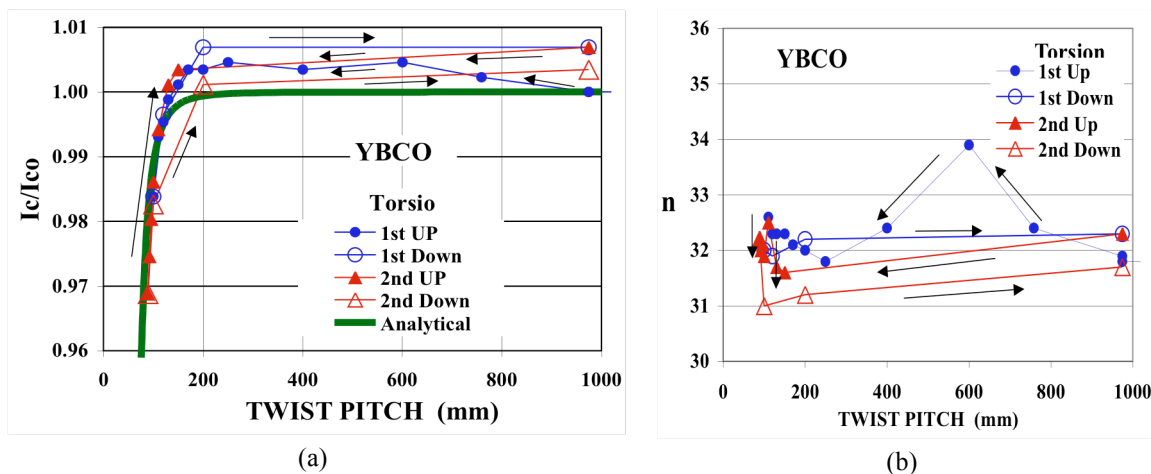(a)   (b)

FIGURE 3. Critical current test results of YBCO obtained under various torsional twists; (a) The normalized critical currents with a curve calculated with the analytical mode, and (b) The n-values.
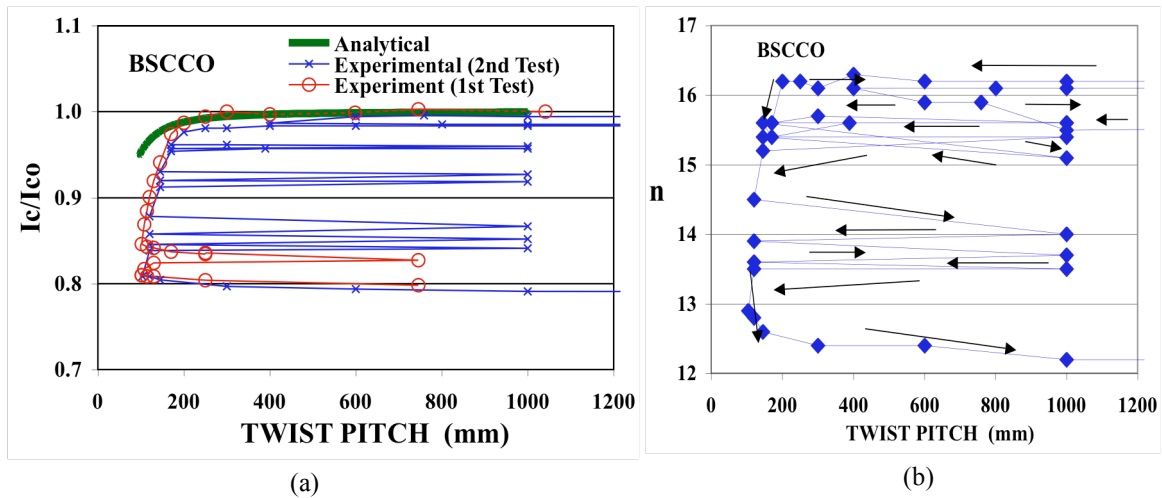
(a) (b)

FIGURE 4 (a) Normalized critical currents as a function of the twist pitch. Two BSCCO tape tests are shown along with a curve of the analytical model. (b) The n-values of the 2nd sample.

$$
\begin{aligned}
I_c/I_o &= \exp(70\ \varepsilon_x) & &\text{for } \varepsilon_x < 0 \\
I_c/I_o &= \exp\{-(400\text{-}12.8)\ \varepsilon_x - 400 \times 0.004\} & &\text{for } 0 < \varepsilon_x < 0.004 \qquad (15) \\
I_c/I_o &= \exp(400\ \varepsilon_x) & &\text{for } 0.004 < \varepsilon_x
\end{aligned}
$$

These equations were selected to reflect the manufacturer's general specification values of 5% degradation at 0.4% strain for the BSCCO-2223 tapes.

The experimental results depart sharply from the analytical line below the twist pitch of 200 mm as seen in FIGURE 4. In the analytical model the plastic yielding of the tape was not considered. However, the tested tapes showed clearly permanent deformation due to the applied twists. As mentioned earlier, the maximum shear stress occurs at the tape center surface. Therefore, the center area of the tape, whose strains is compressive, could be yielded more than other area of the tensile strains. Consequently the actual compressive strain could be larger than the calculated values, therefore one can expect that the critical current degradation rapidly increases with twist pitch below 200 mm, corresponding to the yielding phenomena.

DISCUSSION

The critical currents of YBCO tape of the 4 mm width were not degraded by twisting of up to a 200 mm twist-pitch. Below 130 mm twist-pitch the critical currents degraded very sharply as seen in FIGURE 3. At 90 mm twist-pitch the critical current degraded by 3%, but no permanent degradation was observed when the twist was released. The theoretical curve obtained equation (13) in FIGURE 3a agreed very well with the experimental results. On the other hand, the critical currents of BSCCO tapes of 3 mm width with a 35 µm stainless steel reinforcement on the both sides were degraded at 200 mm twist-pitch by about 2%, and then sharply degraded with increasing twist pitch. For a 120 mm twist pitch, the critical current degraded by 20%. The degradation of the BSCCO tape due to the torsion was not recovered after removing of the torsion. We conclude that 2G YBCO tapes are very strong to mechanical twists, but 1G BSCCO-2223 tapes permanently degrade with twisting.

The longitudinal strain model discussed above describes very well experimental results of the critical currents of a twisted tape. In the model, the critical current of a twisted tape have been calculated with equations (5) and (13) using the reported

dependence of the critical current with axial strain. Twist effects on the critical current of a conventional power cable composing lapped multi tapes have been shown to be evaluated from that of a twisted single tape.

The critical current of the HTS tape conductor composing twisted stacked-tapes can be also evaluated from that of a twisted single tape. Recently the field angle degradation (critical current anisotropy) of YBCO tapes has been improved using a REBCO film technique substituted with Gd and Zr [5, 14]. Therefore a twisted YBCO stacked-tape cable can be conceived for compact high-current power conductors and high-current high-field conductors. A stacked and twisted conductor of 7 mm diameter composed of the 40 tapes may carry up to approximately 3 kA at 77 K with self field and 4.5 kA at 15 T at 4.2 K. A three-stage 9-conductor cable (3x3) of 32 mm diameter may provide 25 kA at 77 K at self field and 40 kA at 15 T at 4.2 K. In the same conductor diameter, it will be possible to make a12-conductor cable with a single stage cabling of 30 kA at 77 K at self field and 50 kA at 4.2 K at 15 T.

CONCLUSIONS

Analysis of the critical current of HTS tapes under torsional twisting strains has been carried out. Torsional twist effects on a thin HTS tape has been found to be well described by the longitudinal strain model taking account of the resulting compressive strain accompanied with the tensile longitudinal strain due to a torsional twist. The critical current of a twisted tape is obtained for the integration of the critical currents of a function of the longitudinal strain using axial strain test data of the tape. The model analysis results are agreed with experimental results of BSCCO and YBCO tapes.

The critical current of a tape of both lapped-tape and stacked-tape cables is found to be described with the critical current equation developed for a twisted single tape having the same twist pitch.

Twisted stacked tape conductors will be attractive to various applications of high power transmission lines, mainly DC cables, and high current conductors of magnets for medical applications such as compact synchrocyclotron and MRI, SMES, and other electrical devices (transformer, fault current limiter and generators).

REFERENCES

1. Maguire, J.F. et al., *IEEE Trans. Appl. Supercond.*, **17**, pp. 2034-2037 (2007).
2. Yamaguchi, S. et al, *Journal of Physics: Conference Series*, **97,** 012290 (2008).
3. Long, N.J., et al., *Journal of Physics: Conference Series*, **97,** 012280 (2008).
4. Lee, P., http://magnet.fsu.edu/~lee/plot/plot.htm.
5. Hazelton, D.W. et al., *IEEE Trans. Appl. Supercond.*, presented at ASC, Chicago, 2008.
6. Jin, J.X. et al, *IEEE Trans. Appl. Supercond.*, **9**, pp. 138-141 (1999).
7. Shin, H.S. et al., *Physica C*, 392-396, pp. 1162-1166 (2003).
8. Shin, H.S. et al., *IEEE Trans. Appl. Supercond.*, **17**, pp. 3274-3277 (2007).
9. Timoshenko, S., *Strength of Materials II*, 3rd ed., Van Nortrand Reinhold Co., N. Y., 1958, p. 288.
10. Green, A.E., Proc. R. Soc. Lond., Ser. A, 154, pp. 430-455 (1936).
11. Timoshenko, S. et al., *Theory of Elastidity*, 3rd ed., Van Nortrand Reinhold Co., N. Y., 1934, p. 308.
12. P.C. Michael et al., *IEEE Trans. Appl. Supercond.*, **13**, pp. 1620-1623 (2003).
13. http://superpower-inc.com: 2G Strain effect measured by Danko van der Laan, NIST.
14. Haken, B.T. et al., *IEEE Trans. Mag.*, **32**, pp. 2720-2723 (1996).
15. http://superpower-inc.com: 2G field data obtained by Y. Zhang, M. Paranthaman, and A. Goyal, ORNL.